Cu/Al_2O_3 catalysts for soot oxidation: Copper loading effect.

F. E. López-Suárez, A. Bueno-López*, M.J. Illán-Gómez.

Inorganic Chemistry Department, University of Alicante. Ap. 99, E-03080 Alicante (Spain)

Abstract

Cu/Al_2O_3 catalysts with metal loading from 0.64 to 8.8 wt. % have been prepared and characterised by different techniques: N_2 adsorption at -196ºC (BET surface area), ICP (Cu loading), XRD, selective copper surface oxidation with N_2O (Cu dispersion), TPR-H_2 (redox properties), and XPS (copper surface species). The catalytic activity for soot oxidation has been tested both in air and NOx/O_2. The activity in air depends on the amount of easily-reduced Cu(II) species, which are reduced around 275ºC under TPR-H_2 conditions. The amount of the most active Cu(II) species increases with the copper loading from Cu_1% to Cu_5% and remains almost constant for higher copper loading. In the presence of NOx, the first step of the mechanism is NO oxidation to NO_2, and the catalytic activity for this reaction depends on the copper loading. For catalysts with copper loading between Cu_1% and Cu_5%, the catalytic activity for soot oxidation in the presence of NOx depends on NO_2 formation. For catalysts with higher copper loading this trend is not followed because of the low reactivity of model soot at the temperature of maximum NO_2 production. Regardless the copper loading, all the catalysts improve the selectivity towards CO_2 formation as soot oxidation product both under air and NOx/O_2.

Keywords: Soot; NOx; alumina; copper catalyst.

* Corresponding author: A.Bueno López (agus@ua.es)
Inorganic Chemistry Department, University of Alicante. Ap. 99, E-03080 Alicante (Spain)

1.- Introduction.

Among the different catalytic after-treatment technologies proposed for soot removal in diesel exhausts, the so-called CRT (Continuously Regenerating Trap) seems to be the most satisfactory at this moment [1], especially for heavy-duty diesel applications. This system consists of a Pt catalyst for NO oxidation to NO_2, which is more oxidizing than NO and O_2. The soot filter located downstream is continuously regenerated by soot oxidation to CO_2 using the previously produced NO_2.

However, the CRT system presents several drawbacks that need improvements, motivating fundamental and applied research work. NOx removal over a CRT catalyst is somewhat less than 10% [1], and an additional system for NOx removal is required. It is also reported that soot oxidation is strongly inhibited by the presence of SO_2, so the CRT technology could not be introduced until low sulphur diesel fuel became available [1]. In addition, because of the high price of noble metals new active components based on non-noble metals are desired.

Looking for new, cheaper and efficient catalytic components [2], several alkali (Na, K, Rb), alkali-earth (Ca), transition (Fe, Co, Ni, Cu, Cr, Zr) and rare-earth (Ce) metals were loaded on carbonaceous materials and the catalytic combustion was tested under NOx/O_2. Among the metals studied, the lowest light-off temperatures were obtained with Rb and Cu [2]. In the same line, Bloom et al. [3] compared Fe, Cu and Ce fuel additives and found that only copper could efficiently regenerate the filter. G. Mul et al. [4] also screened a number of metal chlorides (Ba, Ca, Fe, Bi, Hg, Co, Mo, Ni, Cu, and Pb) for catalytic oxidation of model soot, concluding that those based on Pb and Cu are the most active. However, they reported that the application of metal chlorides as catalysts for diesel soot oxidation is questionable, because the loss of activity by evaporation or decomposition of the active species is a severe problem [4].

A number of copper-containing multi-component catalysts have also demonstrated to be active for soot oxidation, such us CuO/CeO_2 [5], copper-loaded MFI zeolite [6], Al_2O_3-[7] and CeO_2-[8] supported copper vanadates, $CuO/Nb_2O_5/SiO_2$-Al_2O_3 [9], copper-containing perovskites ($La_{0.8}K_{0.2}Cu_{0.05}Mn_{0.95}O_3$ [10] and

$La_{0.8}Sr_{0.2}Mn_{0.5}Cu_{0.5}O_3$ [11]) and bimetallic Cu/K active phases supported on ZrO_2 [12], Al_2O_3 [13] and beta zeolite [14], among others.

The lower price of copper in comparison to noble metals makes this transition metal a promising candidate for practical utilization in diesel soot removal. Some authors have also reported that certain copper-containing catalysts ($La_{0.8}K_{0.2}Cu_xMn_{1-x}O_3$ [10], $Cu/K/Al_2O_3$ [13] and Cu/K/beta zeolite [14]) are able to promote the simultaneous removal of NOx and soot. Sulphur resistance seems to be another benefit of copper catalysts, since S. Mosconi et al. [15] have observed that a Cu/Al_2O_3 catalyst tested for soot oxidation under NOx/O_2 does not suffer deactivation by SO_2 poisoning, even under severe conditions such as 1000 ppm SO_2/600ºC.

There have been proposed two main mechanisms through a metal oxide-catalysed soot oxidation could proceed [4], and both could be valid for copper catalysts. One of them is the reduction/oxidation mechanism (Mars and van Krevelen), where in a first step the metal oxide is reduced by the soot, and in a second step the catalyst is reoxidised by an oxidising gas. The other mechanism is based on a spill-over effect. Oxygen is activated on the surface of a metal oxide, and subsequently transferred to the soot surface where reacts yielding surface oxygen complexes and finally CO and/or CO_2. G. Mul et al. [4] reported that soot oxidation in air catalysed by copper chlorides is based on the latter mechanism. However, the catalytic combustion of copper-loaded char in NOx/O_2 could be explained according to the reduction/oxidation mechanism, as suggest by the XPS analyses of the copper species (including Cu(0), Cu(I) and Cu(II)) detected on fresh and used samples [16]. In both cases, and also considering some other reported studies, it can be concluded that the redox properties of copper play a major role in its catalytic activity for carbon materials oxidation. However, there are several issues that remain unclear, such as the importance of the copper loading and dispersion in the activity of copper catalysts for soot oxidation and/or the relative importance of these two variables in comparison to the redox properties of this metal.

In the case of multi-component catalysts, the role of copper is more difficult to be analysed, and depends on the material considered. As an example, the role of copper on the catalyst $La_{0.8}K_{0.2}Cu_{0.05}Mn_{0.95}O_3$ [10], with perovskite structure, is proposed to be the creation of crystal defects. For copper-vanadium-cerium oxide catalysts, its high

activity for model soot oxidation was attributed to the presence of the V_2O_5 phase, while it is suggested that copper (II) species are responsible for the low CO production [8].

In the current study, a set of Cu/Al_2O_3 catalysts with different metal loading, have been prepared, characterised and tested for soot oxidation both in air and NOx/O_2. The goal of the study is to get insight into the properties of copper that could affect the catalytic activity, including copper loading, copper dispersion, type of surface copper species and copper redox properties.

2.- Experimental.

2.1. Catalysts preparations.

γ-Al_2O_3 from Across (88 m^2/g BET surface area) was impregnated with $Cu(NO_3)_2{\cdot}3H_2O$ water solutions (10 $ml_{solution}/g_{Al2O3}$) of the required concentration to obtain catalysts with different target copper loading (1, 3, 5, 7, 10 and 15 wt.%). Most of the solvent was removed by air bubbling, and once apparently dry, the samples were heated in static air at 110ºC for 12 hours and calcined at 700ºC for 5 hours for nitrate decomposition. The calcinations temperature has been selected taking into account that the complete soot conversion in the catalytic tests performed with NOx/O_2 is reached at 700ºC. The catalysts are denoted by "*Cu_X%*", where "X" indicates the target copper loading.

2.2. Catalysts characterizations.

The catalysts BET surface areas were determined by physical adsorption of N_2 at –196ºC in an automatic volumetric system (Autosorb-6B from Quantachrome) after degassing the samples at 250ºC for 4 hours.

The actual copper loading (*Cu(%)*) of the different catalysts was determined by ICP in a Perkin–Elmer device, model Optimal 3000. For this purpose, the metal was extracted from the catalysts (after mechanical vibration using an ultrasonic bath to remove weakly attached metal particles) by refluxing them in a 6M HCl solution for 8 h.

X-ray difractograms of the catalysts were recorded in a Seifert powder diffractometer, using CuKα radiation. Spectra were registered between 20 and 80º (2θ) with a step of 0.02º and a time per step of 3 seconds.

Temperature Programmed Reduction experiments were carried out with H_2 (TPR-H_2) in a Micromeritics device, model Pulse ChemiSorb 2705. 20 mg of catalyst were heated at 10ºC/min from 25 to 900ºC under a 5%H_2/Ar flow (35 ml/min, P_{total}=1 atm), and the H_2 consumption was monitored with a TCD detector. A CuO reference sample (supplied by Micromeritics) has been used to quantify H_2 consumption.

The Micromeritics device was also used for the estimation of copper dispersion, following the procedure described by Gervasani and Bennici [17]. The method consists of, firstly, the copper oxide reduction with 5%H_2/Ar (15 ml/min) by heating 150 mg of catalyst at 8ºC/min from 25 to 400 ºC, holding the maximum temperature for 30 minutes. Then, the selective oxidation of the copper surface to Cu_2O is performed under 0.53% N_2O/Ar flow (20 ml/min) at 50ºC:

$$N_2O + 2Cu_{surface} \rightarrow Cu_2O_{surface} + N_2 \quad (1)$$

$Cu_2O_{surface}$ is further reduced with 5%H_2/Ar (15 ml/min) by raising the temperature at 20ºC/min from 25 to 1050 ºC, following the H_2 consumption with the TCD detector.

$$H_2 + Cu_2O_{surface} \rightarrow 2Cu_{surface} + H_2O \quad (2)$$

Surface copper is determined considering the stoichiometry of the reaction (2), and the parameter "*Dispersion (%)*" is calculated as the ratio between the amount of surface copper and total copper measured by ICP.

$$\text{Dispersion (\%)} = \frac{Cu_{surface}\,(g)}{Cu_{total}\,(g)} \cdot 100 \quad (3)$$

Once copper loading and dispersion were determined, the surface copper of the catalysts ($Cu_{surface}$ *(%)*) was estimated with the equation (4):

$$\mathrm{Cu_{surface}\ (\%)} = \frac{\mathrm{Cu_{surface}\,(g)}}{\mathrm{Mass\ of\ catalyst\,(g)}} \cdot 100 = \frac{\mathrm{Dispersion\ (\%)} \cdot \mathrm{Cu\ (\%)}}{100} \qquad (4)$$

XPS characterisation was carried out in a VG-Microtech Multilab electron spectrometer using Mg-Kα (1253.6 eV) radiation source. To obtain the XPS spectra, the pressure of the analysis chamber was maintained at $5 \cdot 10^{-10}$ mbar. The binding energy (BE) scale was adjusted by setting the C1s transition at 284.6 eV.

2.3. Catalytic tests.

Catalytic tests were performed in a fixed-bed reactor at atmospheric pressure under a gas flow (500 ml/min) containing synthetic air or 500 ppm NO_x+5%O_2. The model soot used was a carbon black from Cabot (Vulcan XC72). The experiments consisted of heating the soot-catalyst mixtures from 25 to 800 °C at 10 °C/min. The soot-catalyst mixtures contained 80 mg of catalyst + 20 mg of soot + 300 mg SiC, and were prepared with a spatula following the so-called "*loose contact*" procedure [18]. Blank experiments were performed only with the catalysts (without soot) under similar experimental conditions. The gas composition was monitored by specific NDIR-UV (Non Dispersive Infrared Ultra-Violet) gas analyzers for NO, NO_2, CO, CO_2 and O_2 and the soot conversion was determined from CO and CO_2 evolved.

$$-\frac{\mathrm{dm}}{\mathrm{dt}} = \left(\mathrm{CO} + \mathrm{CO_2}\right) \cdot \mathrm{F} \qquad (5)$$

In the equation (5), "m" is the mass of soot, "t" is the reaction time, CO and CO_2 the volumetric fraction of each gas, and F the total gas flow. In all the experiments, the carbon mass balance was obtained by numerical integration of equation 5 and was closed in the range 100–125% of the amount of soot loaded into the reactor. From soot conversion profiles, the parameter "*T50% (ºC)*" has been determined, which is the temperature required to reach 50% soot conversion. In addition, the selectivity towards CO_2 formation with regard to total CO_x emitted was determined by the equation (6):

CO_2 selectivity (%) = $100 \cdot CO_2/(CO + CO_2)$ (6)

The N_2O formation as NO_x reduction product was ruled out in additional experiments followed by gas chromatography using a HP 6890 plus series device. This set-up is described in detail elsewhere [19].

3. Results and discussion

3.1. Characterization of catalysts: copper loading and dispersion.

Table 1 compiles the BET surface area of the different samples along with their copper loading and dispersion, as well as the percentage of copper oxide reduced during TPR-H_2 experiments (to see below). The BET values decrease progressively, as the copper loading increases, from 88 m^2/g for the bare support to 70 m^2/g for the catalyst with the highest copper loading. This is an evidence of the partial blocking of the support surface by copper. As expected, the copper dispersion decreases by increasing copper loading, that is, the particle size of copper increases.

In the Figure 1a, the actual copper loading, as measured by ICP (Cu(%)), is drawn as a function of the target copper loading. All the catalysts contain a lower amount of copper than that expected (target copper loading), that is, values are below the auxiliary line with slope = 1. This means that part of the copper used for the impregnation is not incorporated to the alumina. It has to be underline that the Cu ICP measures was carried out after removing metals particle weakly attached, as indicated in the experimental section. The discrepancy between actual and target copper loading is little for catalysts till 7% loading, but there is a threshold around 9% loading that can not be overcome. It is important to mention that the sample Cu_15% shows heterogeneous appearance, and two types of particles (black and grey, respectively) can be distinguished. We attributed this fact to the presence of copper/copper oxide particles along with the Cu-containing Al_2O_3 particles. Due to this heterogeneity and lack of reproducibility in the preparation, this sample has been rejected for the catalytic tests.

One important feature of a catalyst is the surface population of active sites, which is related with the amount of surface copper on the catalyst. As expected, data in Table 1 show that the copper loading and dispersion follow opposite trends, that is, the higher the copper loading, the lower the copper dispersion. In the Figure 1b, the surface copper is plotted as a function of the copper loading, showing an optimum value around 5% for which a maximum percentage of surface copper is reached.

In the Figure 2, the X-ray powder diffraction patterns of the catalysts are shown. All the XRD patterns show broad diffraction peaks due to poorly microcrystalline γ-alumina. The diffraction peaks corresponding to Cu–containing phases are not observed Cu_1%, Cu_3% and Cu_5% catalysts, in agreement with the high copper dispersion, while the most intense reflections corresponding to CuO (at 2θ values of 35.5 º and 38.8 º) are clearly visible for the catalysts Cu_7% and Cu_10%. The presence of metal oxide clusters with a strong interaction with the support cannot be excluded because their XRD diffraction peaks appear at the same 2θ angles that those of Al_2O_3. The absence of CuO diffraction peaks in some catalysts indicate the formation of finely dispersed copper species on the alumina surface that are not detectable by this technique. Thu, XRD results are in agreement copper dispersion results.

In conclusion, the results discussed in this section indicate that the highest surface copper amount is reached with 5 % copper loading, and with the experimental procedure followed and materials used, it is not possible to reach copper loading higher than 9%.

3.2. Catalytic tests in air.

In the Figure 3, the soot conversion profiles during soot oxidation experiments in air are plotted as a function of temperature and, in the Table 2, the values of the parameter T50% are compiled together with those of CO_2 selectivity determined with the equation (6).

The onset temperature for the uncatalysed combustion in air is 600ºC approximately, and the complete conversion is reached at 775ºC. All the catalysts tested increase the soot combustion rate and shift the conversion profiles to lower

temperatures. The catalytic activity increases with the copper loading from Cu_1% to Cu_5%, but higher copper loading do not improve the catalytic activity. According to these results, it does not make sense to increase the copper loading above 5% for soot oxidation in air. Considering the characterization results discussed in the previous section, the activity in air can not be directly correlated with the copper loading and neither with the surface copper (Figure 1b), because there are catalysts with the same activity but different surface copper (Cu_5%, Cu_7% and Cu_10%). The main characteristic of the copper catalysts affecting their activity in air will be explained in detail afterwards, in the section 3.5. focussed on TPR-H_2 and XPS characterization.

On the other hand, all the copper catalysts improve the selectivity towards CO_2 formation from 36% for the uncatalysed reaction to about 100% for all the copper-catalysed reactions (data in Table 2). Note that CO_2 is the desired soot oxidation product due to the high toxicity of CO. This improvement in CO_2 selectivity could be attributed, in one hand, to the fact that soot combustion takes place at lower temperature, and CO is the thermodynamically preferred product at high temperature. However, the difference between CO_2 selectivity for the uncatalysed (36%) and catalysed reactions (~100%) is too high considering the relatively narrow range of temperatures (600-775ºC) where soot combustion takes place. Therefore, even if the decrease in soot oxidation temperature could affect in some extent the CO_2 selectivity data, it is not the main argument to justify these values. On the other hand, copper-catalysts are active for CO oxidation to CO_2, and this seems to be the main reason of the high selectivity of the catalysts studied towards CO_2 formation. Thus, CO seems to be the primary soot oxidation product, as deduced from the uncatalysed experiments and copper catalyses the oxidation of CO to CO_2 afterwards. The high activity of copper for CO oxidation is well-known, and some authors have proposed Cu-based catalysts as potential candidates to substitute precious metals in CO oxidation catalysts [20].

3.3. Catalytic tests in NO_x/O_2

3.3.1. Soot oxidation.

The effect of NOx in soot oxidation has been studied, and the Figure 4 shows the soot conversion profiles during the experiments performed under NOx/O_2. In the

presence of NOx, the uncatalysed and copper-catalysed reactions take place at lower temperatures than the counterpart reactions in air (Figure 3). Considering the T50% temperatures included in Table 2, there is a shift of around 50ºC to lower temperature in NOx/O_2 in comparison to air. The shift in the light-off temperatures for the catalysed reactions is greater, being around 500ºC for most of the copper-catalysed reactions in NOx/O_2.

Copper loading also has a significant effect on catalytic activity in NOx/O_2, as described for air. For instance, the T50% values (Table 2) decrease progressively from 650 to 596ºC from Cu_1% to Cu_7% respectively. Above this loading there is not additional increase in activity, Cu_7% and Cu_10% showing quite similar behaviour. The catalytic activity of copper in NOx/O_2 can not be correlated with one of the single parameters described in section 3.1 (copper loading, copper dispersion or surface copper), as already discussed for experiments in air, and some other characteristic seems to play the major role. This will be discussed afterwards.

The copper catalysts are also selective for CO_2 formation as soot oxidation product in the presence of NOx (data in Table 2). In fact, CO emission is not detected in any catalytic tests performed under NOx/O_2. This is not the case of the uncatalysed reactions, where the same low CO_2 selectivity (36%) is obtained both under air and NO_x/O_2, supporting that copper is responsible of the high CO_2 selectivity.

3.3.2. NO_x removal.

The NOx removal profiles obtained during the soot oxidation tests are compiled in the Figure 5a, and for proper interpretation of these profiles, the counterpart curves obtained in blank experiments (without soot, only using the catalysts) have been included in the Figure 5b.

The uncatalysed soot oxidation in NOx/O_2 takes place between 500 and 725ºC approximately (see Figure 4). In this range of temperature NOx removal occurs, as observed in the Figure 5a, due to the NOx-C reaction that yields N_2 and CO/CO_2. This reaction takes place simultaneously to the O_2-C combustion, which is the main soot

consumption pathway. For the sake of brevity, the O_2 consumption profiles are not shown.

NOx removal profiles in catalytic combustion experiments are much more complexes than soot oxidation profiles. Regardless the catalyst considered, all the NOx removal profiles reach a maximum value in the range 600-700ºC that must be attributed to NOx reduction by soot. The temperature for this maximum NOx removal decreases as the copper loading increases from Cu_1% to Cu_5%, and it is reached more or less at the same temperature for Cu_5%, Cu_7%, and Cu_10%. This trend is consistent with the trend in soot conversion temperature (see soot conversion profiles in Figure 4 and T50% values in Table 2). The maximum NOx reduction level reached was 11% (for Cu_1%), and therefore, the Cu/Al_2O_3 catalysts studied could not be used for the simultaneous removal of NOx and soot without an additional NOx removal strategy.

The NOx removal profiles obtained with Cu_5%, Cu_7%, and Cu_10% also show a wide shoulder at lower temperatures (around 450ºC), which must be attributed to NOx chemisorption on the catalysts. It is reasonable to assume that between both ranges of temperature (shoulder around 450ºC and maximum at 600-700ºC), both processes (NOx chemisorption and NOx reduction, respectively) could progress together.

The hypothesis of NOx chemisorption on the catalysts around 450ºC was confirmed in experiments performed without soot (Figure 5b), since in this case the NOx removal pathway throughout the NOx-C reaction can be ruled out. NOx removal in blank experiments (without soot) due to chemisorption on the catalysts depends on the copper loading, increasing from Cu_1% to Cu_5% with maximum removal for the latter, and slightly decreasing for Cu_7% and Cu_10%. This trend is the same than that obtained for surface copper in the Figure 1b, and indicates that NOx chemisorption, as expected, is a surface phenomenon.

Comparison between Figures 5a and 5b allows concluding that the copper-catalysed soot combustion decreases the amount of NOx chemisorbed on the catalyst. As an example, NOx removal on the Cu_5% catalyst reaches 15% at 450 ºC in the absence of soot (Figure 5b) while the NOx removal in the presence of soot at the same

temperature is only 3% for this catalyst. This is because the copper surface is involved in both the NOx chemisorption and the catalysed soot oxidation, and therefore, it is expected that the copper fraction involved in the catalysed soot oxidation is not available for NOx chemisorption. The same phenomenon was previously observed for a CeO_2 catalyst [21]. Related with this fact, Pisarello et al. [22] also concluded that the formation of stable nitrate species on a K/Ba/CeO_2 catalyst inhibits the soot combustion reaction.

One important issue that must be considered in catalysed soot oxidation under NOx/O_2 is the formation of NO_2, which is much more oxidising than NO and O_2, as mentioned. NO is the main component of NOx in a real diesel exhaust, and it is also in the experimental set up used for the catalytic tests. In the Figure 6, the NO_2 percentage, on the basis of the NO + NO_2 level, is plotted as a function of temperature for the blank experiments. Despite NO_2 is the thermodynamically stable nitrogen oxide at low temperature, the conversion of NO to NO_2 presents kinetic restrictions, and the copper catalysts raise the NO oxidation rate. For instance, NO_2 is detected from 300ºC with the catalyst Cu_10%, reaches a maximum level of 14% at 465ºC, and then decreases following thermodynamics. The delay between thermodynamics and experimental NO_2 profiles must be attributed to the time required for the gas to go from the reactor to the analysers. The maximum NO_2 concentration reached depends on the copper loading, and as a general trend, the higher the loading the higher the activity for NO oxidation to NO_2. These results suggest that there is a certain relationship between the catalytic activity of the copper catalysts for NO oxidation to NO_2 and for soot oxidation, which is due to the high soot oxidation capacity of NO_2. For example, the trend in T50% temperatures (Table 2) for Cu_1%, Cu_3% and Cu_5% (650, 623, and 610ºC, respectively) is related to the trend of the maximum NO_2 level reached in Figure 6 (1, 4, and 8 %, respectively).

However, it is surprising that the catalytic activity for soot combustion of Cu_7% and Cu_10% are almost the same (see profiles on Figure 4 and T50% values on Table 2) while the latter is much more effective for NO_2 formation (Figure 6). This could be attributed to the fact that the maximum NO_2 level is reached around 450ºC for both catalysts, and the reactivity of soot at this temperature is low (see Figure 4). In other words, NO_2 is not effective for soot oxidation at 450 ºC, at least for the model soot

used in this study. Most probably, the rate limiting step at 450ºC is the decomposition of the oxygen complexes formed on the soot surface upon NO_2 oxidation, but not the oxidation of the carbon surface by NO_2.

The relationship between the temperature required by each catalyst to reach the maximum NO_2 level in blank experiments (Figure 6) and the T50% temperatures determined in the catalytic tests (Table 2) is depicted in Figure 7. Previous discussion is confirmed; a linear trend is observed for Cu_1%, Cu_3% and Cu_5%. In this case, the soot oxidation depends directly on the NO_2 production, which is kinetically controlled by the catalysts. For the catalysts Cu_7% and Cu_10% this trend is not followed because of the low reactivity of the model soot at the temperature of maximum NO_2 production. In fact, it has been probed that using a more reactive model soot (Printex-U), Cu_7% and Cu_10% catalysts follow the observed trend.

3.5. TPR-H_2 and XPS characterization.

In this section, the redox properties of copper are studied by TPR-H_2, and the surface copper species are evaluated by XPS.

The TCD signal profiles obtained in the TPR-H_2 experiments with the set of copper catalysts are drawn in the Figure 8. All the catalysts consumed H_2 in these tests because of the reduction of copper oxide. As expected, the higher the copper loading, the higher the H_2 consumption. The percentage of copper oxide reduced during these experiments has been estimated from H_2 consumption, considering that Cu(II) is the copper specie reduced, and the data obtained are included in the Table 1. Except for Cu_1%, all the catalysts reach near 100% copper reduction. This confirms that the assumption is right and supports that Cu(II) is reduced but not Cu(I) (if Cu(I) were the main copper oxide specie, values around 50% would be expected). Additionally, it is possible to conclude that the presence of metallic copper is minor or null in all the catalysts, except in Cu_1%.

Most of the TCD signal profiles (Figure 8) show two peaks, indicating that copper oxide species with different redox behaviour are present. A peak appears at 275ºC for most catalysts, and it can be attributed to Cu(II) species that are easily

reduced. This peak is probably due to the reduction of a well dispersed CuO phase. The maximum intensity of this peak increases significantly from Cu_1% (null) to Cu_5%, and then slightly for higher copper loading, This trend is similar to that described in the catalytic tests in air (Figure 3), suggesting that the catalytic activity is related to the amount of Cu(II) that is easily reduced. Another peak appears above 300ºC (the right temperature depends on the copper loading) corresponding to less-reducible copper oxide. This high temperature peak can be related to the reduction of larger CuO particles. The maximum intensity of the latter peak increases with the copper loading and the sequence is different to that of the copper dispersion (see data on Table 1). Similar TPR-H_2 profiles of CuO/Al_2O_3 materials has been reported by other authors for different copper catalysts (CuO/Al_2O_3, CeO_2/Al_2O_3, Cu/CeO_2-Al_2O_3) [24] who suggested that the redox properties of CuO are affected by the interaction with alumina and that small CuO clusters and/or isolated Cu^{2+} ions are reduced at lower temperature than larger CuO particles [25].

It is important to take into account that, considering the percentage of copper reduced in TPR-H_2 experiments (data in Table 1), the catalyst Cu_1% could also contain a certain amount of metallic copper along with the copper oxide species. The metallic copper would not contribute to the TCD signal in TPR-H_2 experiments since it would be already reduced. In order to analyse this possibility, the catalysts surface was characterised by XPS following the Cu $2p^{3/2}$ transition. As an example, the profiles corresponding to the catalysts Cu_1% and Cu_3% are included in the Figure 9a and 9b, respectively. The broad profiles can be deconvoluted in three different peaks with maxima at 932.0, 933.5 and 935.1 eV. Reduced copper species, such as metallic copper and Cu_2O, usually appear below 933 eV and CuO typically appears with binding energies higher than 933 eV [23]. The identification of two different CuO species by XPS (at 933.5 eV and 935.1 eV) is consistent with the TPR-H_2 profiles (Figure 8), where two copper oxide species with different reducibility are also identified.

The copper species distribution is different for each catalyst. For instance, the area of the peak at 935.1 eV is low for Cu_1% (Figure 9a) while the area of the peak at 932.0 eV is low for Cu_3% (Figure 9b). This means that copper on Cu_1% is more reduced than on Cu_3%. In order to analyse these differences, the area under the different peaks has been quantified for all the catalysts, and the corresponding

percentages have been then calculated as a function of the total area of the $2p^{3/2}$ transition profiles. In the Figure 10, these percentages are drawn against the copper loading of the catalysts. As mentioned, Cu_1% presents the highest contribution of the most reduced copper species, with 43% of copper appearing with binding energy at 932.0 eV and only 16% with binding energy at 935.1eV corresponding to the most oxidised copper specie. This explains the low intensity of the TCD signal obtained in the TPR-H_2 experiment of Cu_1% (Figure 8), and the low percentage of copper reduced in this catalyst (Table1). In the catalyst Cu_1%, copper is quiet reduced and it does not consumes H_2. With the only exception of Cu_1%, the remaining catalysts present quite similar surface copper species distribution, and not significant differences are appreciated in Figure 10 among them. All the catalysts, except Cu_1%, present around 80 % CuO, calculated as the sum of the 933.5 eV and 935.1 eV contributions. This confirms that there is not important missing information in the TPR-H_2 profiles due to the presence of significant amounts of reduced copper species.

As a summary, the results presented in this study allow concluding that the most active copper species for catalytic soot oxidation in air is the easily-reduced Cu(II) specie, which is reduced around 275ºC under TPR-H_2 conditions. On the contrary, less reducible Cu(II) (reduced under TPR-H_2 conditions above 300ºC) and reduced copper species present lower activity. The amount of the most active Cu(II) species increases significantly with the copper loading from Cu_1% to Cu_5% and slightly for higher copper loading. This is consistent to the catalytic activity trend for soot oxidation in air, and supports the hypothesis of the redox mechanism. In the presence of NOx, the mechanism is more complicated. The first step seems to be the NO conversion to NO_2, and the catalytic activity for this reaction depends on the copper loading. For catalysts with copper loading between Cu_1% and Cu_5%, the catalytic activity for soot oxidation in the presence of NOx depends on NO_2 formation, and NO_2 formation is kinetically controlled by these catalysts. For catalysts with higher copper loading this trend is not followed because of the low reactivity of the model soot used at the temperature of maximum NO_2 production.

4. Conclusions

In this study, Cu/Al_2O_3 catalysts have been prepared by wet impregnation, characterised, and tested for soot combustion in air and NOx/O_2, and the following conclusions can be summarised:

- The activity of the copper catalysts for soot oxidation in air depends on the amount of easily-reduced Cu(II) species, which are reduced around 275ºC under TPR-H_2 conditions. The amount of the most active Cu(II) species increases significantly with the copper loading from Cu_1% to Cu_5% and slightly for higher copper loading.

- In the presence of NOx, the first step of the mechanism seems to be the NO oxidation to NO_2, and the catalytic activity for this reaction depends on the copper loading. For catalysts with copper loading between Cu_1% and Cu_5%, the catalytic activity for soot oxidation in the presence of NOx depends on NO_2 formation. For Cu_7% and Cu_10% this trend is not followed because of the low reactivity of the model soot used at the temperature of maximum NO_2 production.

- A certain NOx reduction occurs along with the copper-catalysed soot combustion, but the maximum reduction level reached with the studied catalysts was 11%, not being high enough for a practical use.

- All the copper catalysts tested improved the selectivity towards CO_2, as soot oxidation product, from 36% for the uncatalysed reaction to 100% for the catalysed reactions. This behaviour is observed both under air and NOx/O_2.

Acknowledgements.

The authors thank the financial support of the MEC (project CTQ2005-01358), and FELS thanks University of Alicante (International Cooperation Office) his thesis grant.

Literature

[1] M. V. Twigg. Appl. Catal. B 70 (2007) 2–15

[2] A. Bueno-López, J.M. Soriano-Mora, A. García-García. Catal. Commun. 7 (2006) 678–684

[3] R.L. Bloom, N.R. Brunner, S.C. Schroeer, SAE paper 970180, 1997.

[4] G. Mu1, F. Kapteijn, J. A. Moulijn. Appl. Catal. B 12 (1997) 33-47.

[5] X. Wu, Q. Liang, D. Weng, Z. Lu. Catal. Commun. 8 (2007) 2110–2114.

[6] Y. Teraoka, K. Kanada, H. Furukawa, I. Moriguchi, S. Kagawa. Chem. Letters 7 (2001) 604-605.

[7] C. Badini, G. Saracco, V. Serra. Appl. Catal. B 11 (1997) 307-328

[8] R. Cousin, S. Capelle, E. Abi-Aad, D. Courcot, A. Aboukaïs. Appl. Catal. B 70 (2007) 247–253.

[9] V. S. Braga, F. A.C. Garcia, J.A. Dias, S. C.L. Dias. J. Catal. 247 (2007) 68–77.

[10] X. Peng, He Lin, W. Shangguan, Z. Huang. Catal. Commun. 8 (2007) 157–161.

[11] S. Wisniewski, J. Belkouch, L. Monceaux. C. R. Acad. Sci. Paris, Serie IIc, Chimie: Chemistry 3 (2000) 443–450.

[12] H. Laversin, D. Courcot, E.A. Zhilinskaya, R. Cousin, A. Aboukaïs. J. Catal. 241 (2006) 456–464.

[13] N. Nejar, M.J. Illán-Gómez. Appl. Catal. B 70 (2007) 261–268.

[14] N. Nejar, M.J. Illán-Gómez. Catal. Today 119 (2007) 262–266.

[15] S. Mosconi, I.D. Lick, A Carrascull, M I. Ponzi, E. N. Ponzi. Catal. Commun. 8 (2007) 1755–1758.

[16] M.J. Illán-Gómez, E. Raymundo-Piñero, A. García-García, A. Linares-Solano, C. Salinas-Martínez de Lecea. Appl. Catal. B 20 (1999) 267-275.

[17] A. Gervasini, S. Bennici 2005. Appl. Catal. A 281 (2005) 199–205.

[18] J.P.A. Neeft, O. P. van Pruissen, M. Makkee, J.A. Moulijn, Appl. Catal. B 12 (1997) 21-31.

[19] A. Bueno-López, J.A. Caballero, A. García-García, Energy Fuels 16 (2002) 1425-1428.

[20] F.H.M. Dekker, M.C. Dekker, A. Bliek, F. Kapteijn, J.A. Moulijn. Catal. Today 20 (1994) 409-422.

[21] I. Atribak, I. Such-Basáñez, A. Bueno-López, A. García-García. J. Catal. 250 (2007) 75–84.

[22] M.L. Pisarello, V. Milt, M.A. Peralta, C.A. Querini, E.E. Miró. Catal. Today 75 (2002) 465–470.

[23] www.lasurface.com

[24] E. Moretti, M. Lenarda, L. Storaro, A. Talon, T. Montanari, G. Busca, E. Rodríguez, A. Jimeénez, M. Turco, G. Bagnasco. Appl. Catal. A 335 (2008) 46–55.

[25] J.Z. Shyu, W.H. Weber, H.S. Ghandi, J. Phys. Chem. 92 (1988) 4964.

Figure captions

Figure 1. (a) Relationship between target and actual (ICP-measured) copper loading (Cu(%)) and (b) surface copper as a function of actual copper loading (Cu(%)).

Figure 2. XRD patterns of the Cu/ Al_2O_3 catalysts.

Figure 3. Soot conversion profiles in catalytic tests performed under air.

Figure 4. Soot conversion profiles in catalytic tests performed under NOx/O_2.

Figure 5. NOx removal profiles in catalytic tests performed under NOx/O_2. (a) With soot and (b) without soot (blank experiments).

Figure 6. NO_2 percentage in catalytic tests performed under NOx/O_2 without soot.

Figure 7. Relationship between temperature of maximum NO_2 formation and T50% in catalytic tests.

Figure 8. Catalysts characterization by TPR-H_2.

Figure 9. XPS characterization of the Cu $2p^{3/2}$ transition for the catalysts (a) Cu_1% and (b) Cu_3%.

Figure 10. Quantification of the different copper species from the deconvoluted XPS-peak areas as a function of actual copper loading (Cu(%)).

Table 1. Samples characterization.

Sample	BET (m^2/g)	Cu (%)	Dispersion (%)	Copper reduced in H_2-TPR (%)*
Al_2O_3	88	-	-	-
Cu_1%	85	0.6	76	49
Cu_3%	82	2.3	59	100
Cu_5%	80	4.6	52	98
Cu_7%	78	6.5	30	92
Cu_10%	72	8.8	16	100
Cu_15%	70	9.4	14	-

*It has been assumed Cu(II) reduction according to the reaction $CuO + H_2 \rightarrow Cu + H_2O$

Table 2. Temperature for 50% soot conversion (T50% (ºC)) and CO_2 selectivity (%) in catalytic tests under air and NO_x/O_2 mixture.

Catalyst	**T50% (ºC) Reaction under air**	**CO_2 selectivity (%) Reaction under air**	**T50% (ºC) Reaction under NO_x/O_2**	**CO_2 selectivity (%) Reaction under NO_x/O_2**
None	715	36	665	36
Cu_1%	692	95	650	100
Cu_3%	679	100	623	100
Cu_5%	666	100	610	100
Cu_7%	665	100	596	100
Cu_10%	664	100	600	100

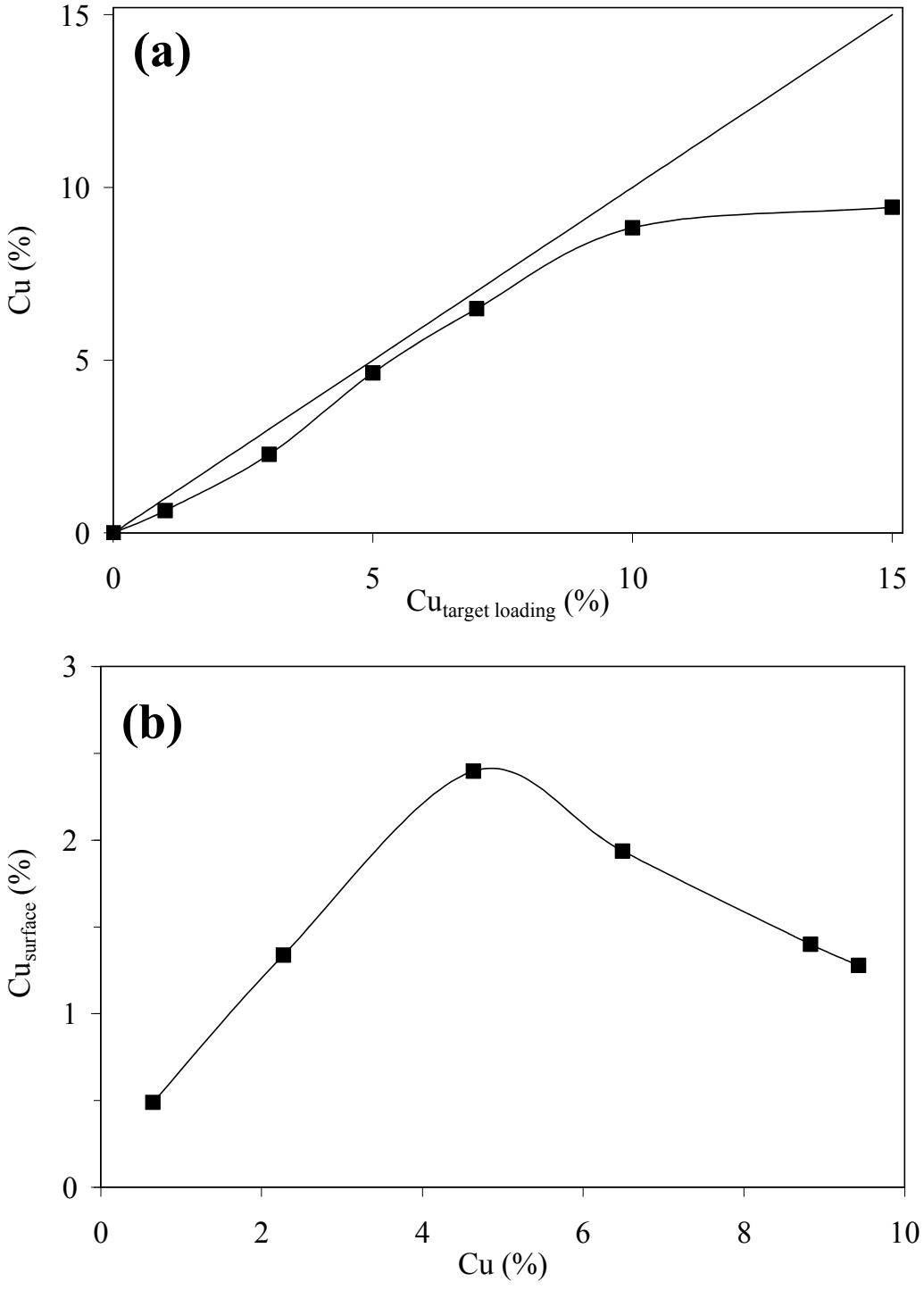
(a)
15
10
5
0
Cu (%)
0
5
10
15
Cu target loading (%)
(b)
3
2
1
0
Cu surface (%)
0
2
4
6
8
10
Cu (%)

Figure 1.

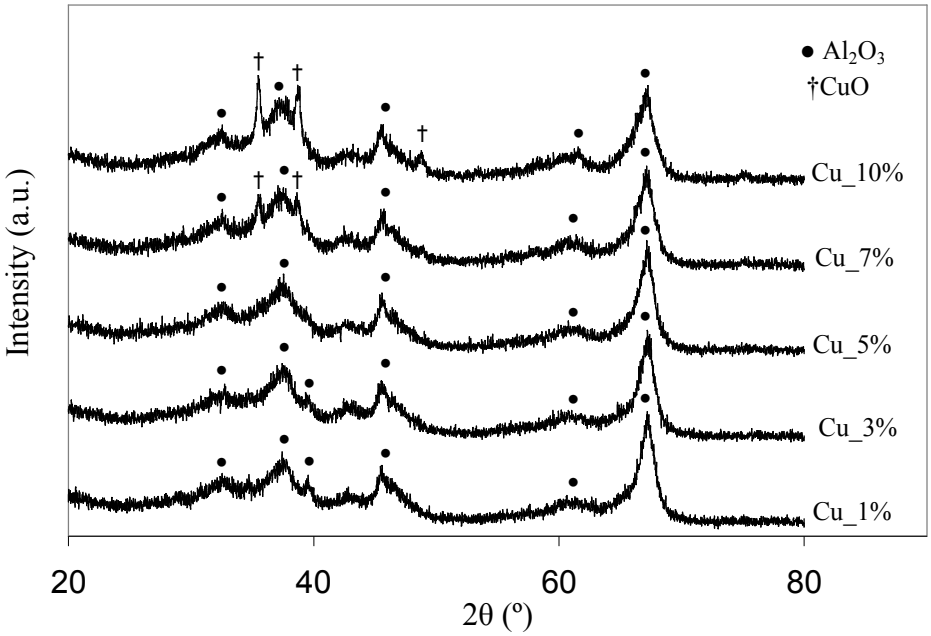

Figure 2.

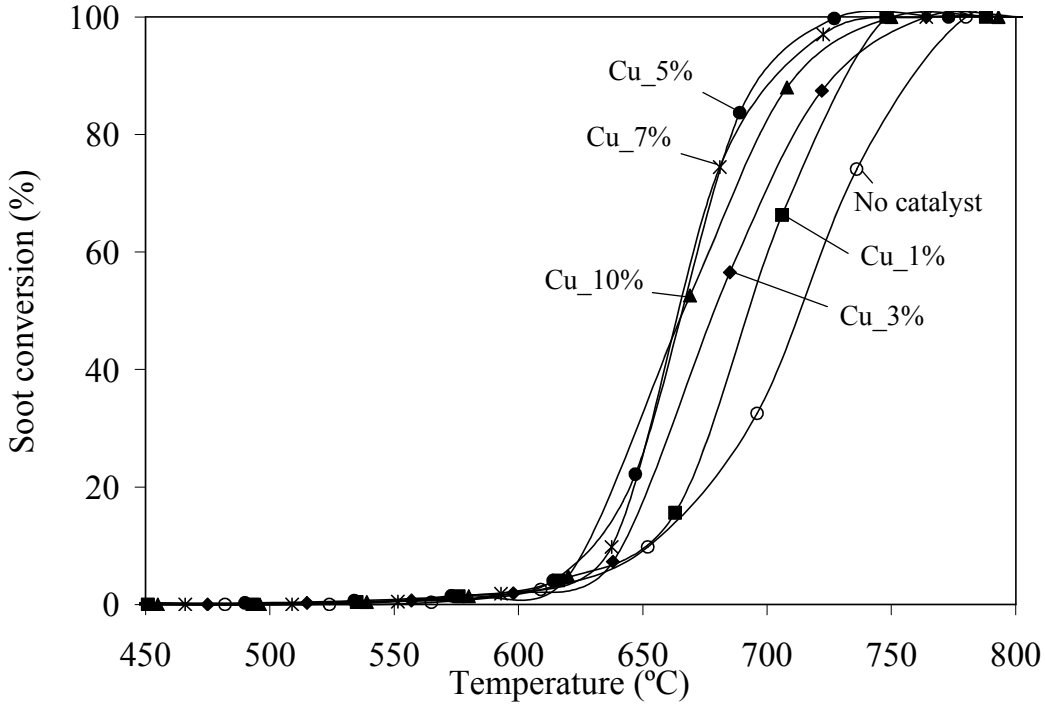
100
80
60
40
20
0
Soot conversion (%)
450
500
550
600
650
700
750
800
Temperature (ºC)
Cu_5%
Cu_7%
No catalyst
Cu_1%
Cu_10%
Cu_3%

Figure 3.

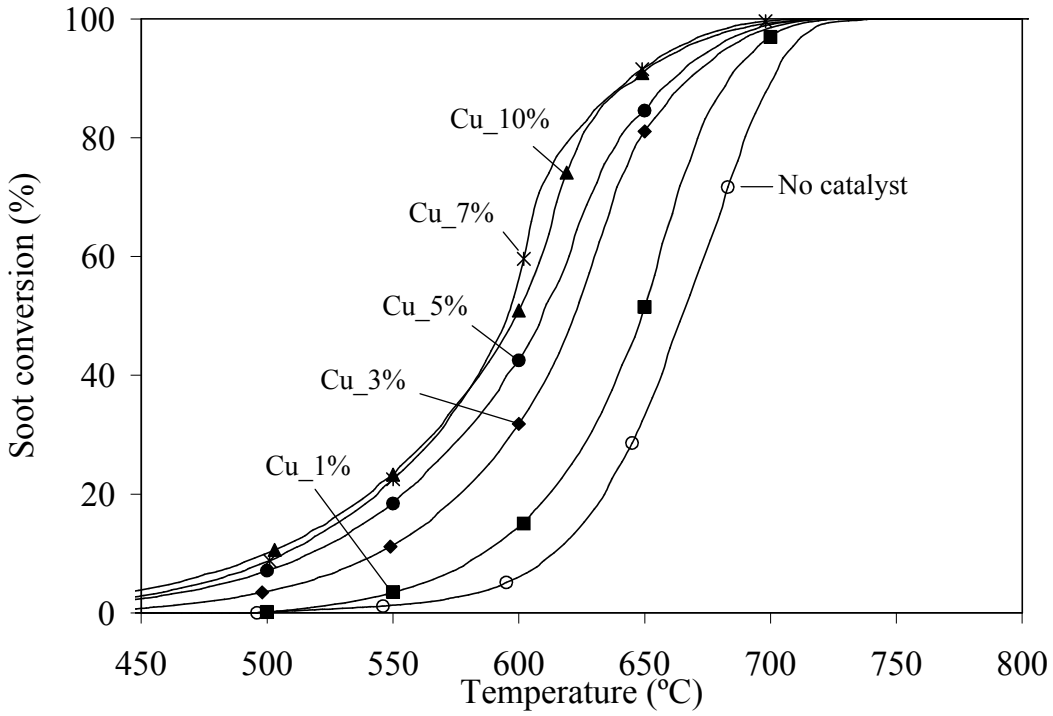
100
80
60
40
20
0
Soot conversion (%)
450
500
550
600
650
700
750
800
Temperature (°C)
Cu_10%
Cu_7%
Cu_5%
Cu_3%
Cu_1%
No catalyst

Figure 4.

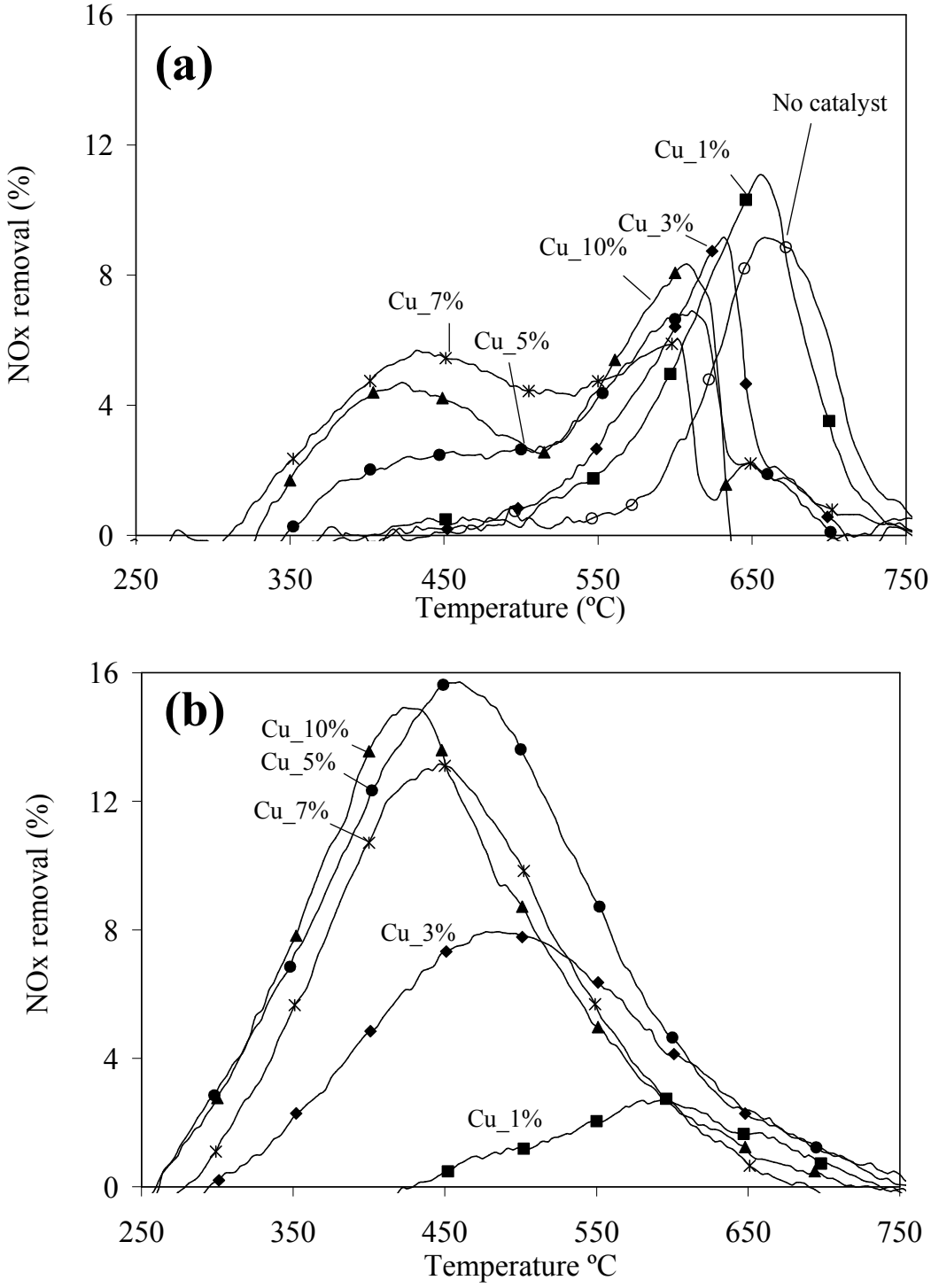
(a)
NOx removal (%)
Temperature (ºC)
No catalyst
Cu_1%
Cu_3%
Cu_10%
Cu_7%
Cu_5%
(b)
NOx removal (%)
Temperature ºC
Cu_10%
Cu_5%
Cu_7%
Cu_3%
Cu_1%

Figure 5.

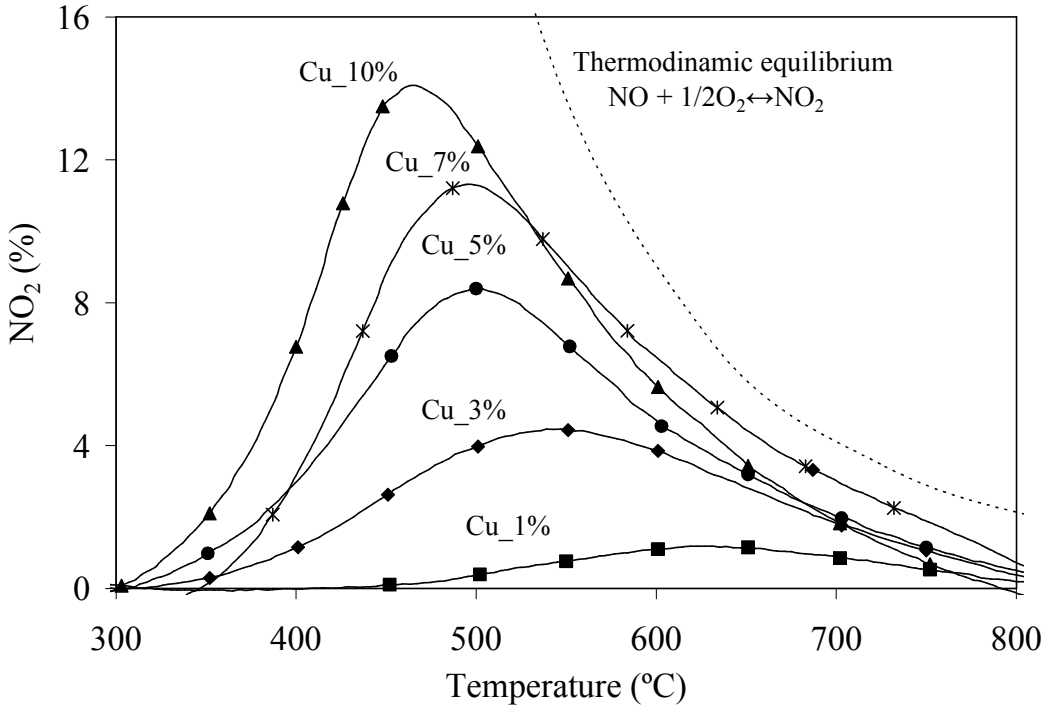
16
12
8
4
0
NO_2 (%)
300
400
500
600
700
800
Temperature (ºC)
Cu_10%
Cu_7%
Cu_5%
Cu_3%
Cu_1%
Thermodinamic equilibrium
$NO + 1/2O_2 \leftrightarrow NO_2$

Figure 6.

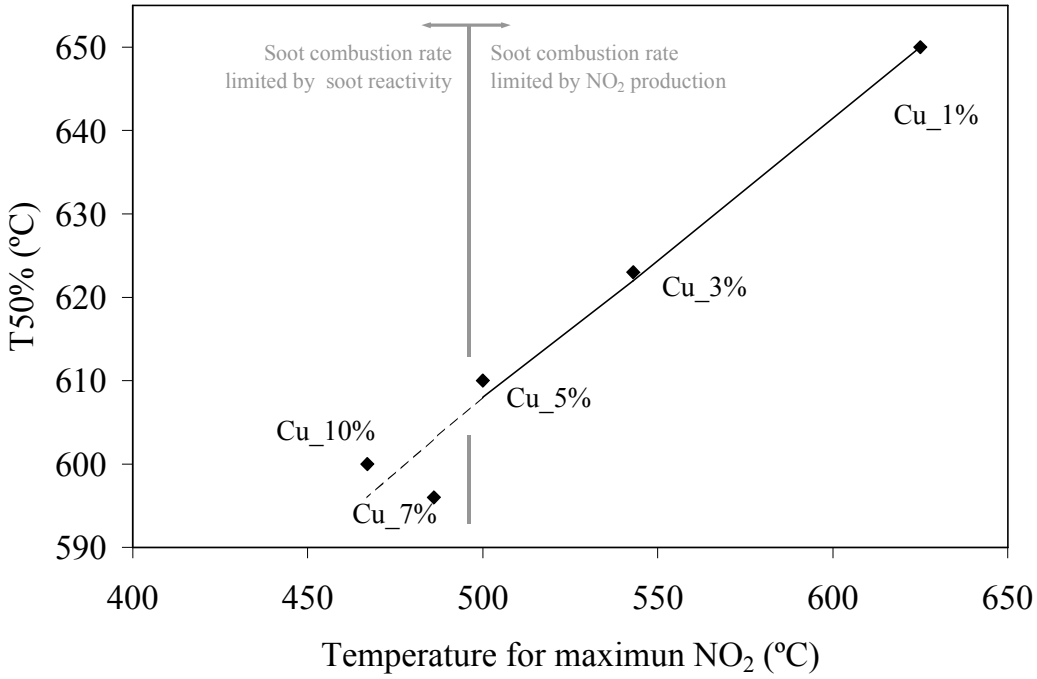
Soot combustion rate
limited by soot reactivity
Soot combustion rate
limited by NO2 production
Cu_1%
Cu_3%
Cu_5%
Cu_10%
Cu_7%
650
640
630
620
610
600
590
T50% (ºC)
400
450
500
550
600
650
Temperature for maximun NO2 (ºC)

Figure 7.

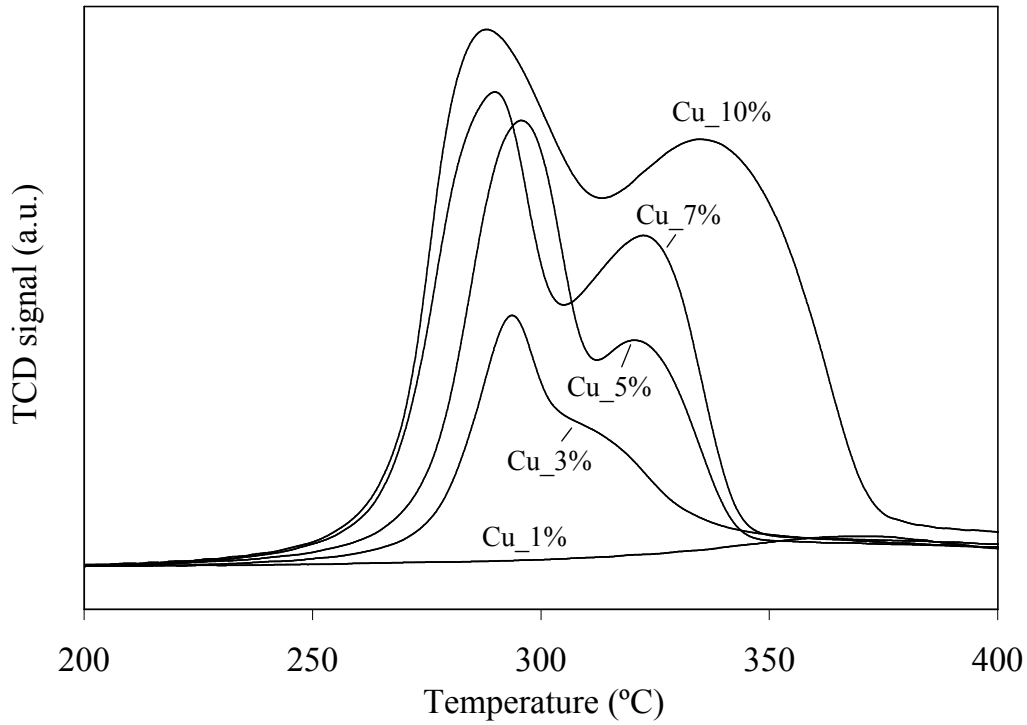
Cu_10%
Cu_7%
Cu_5%
Cu_3%
Cu_1%
TCD signal (a.u.)
200
250
300
350
400
Temperature (ºC)

Figure 8.

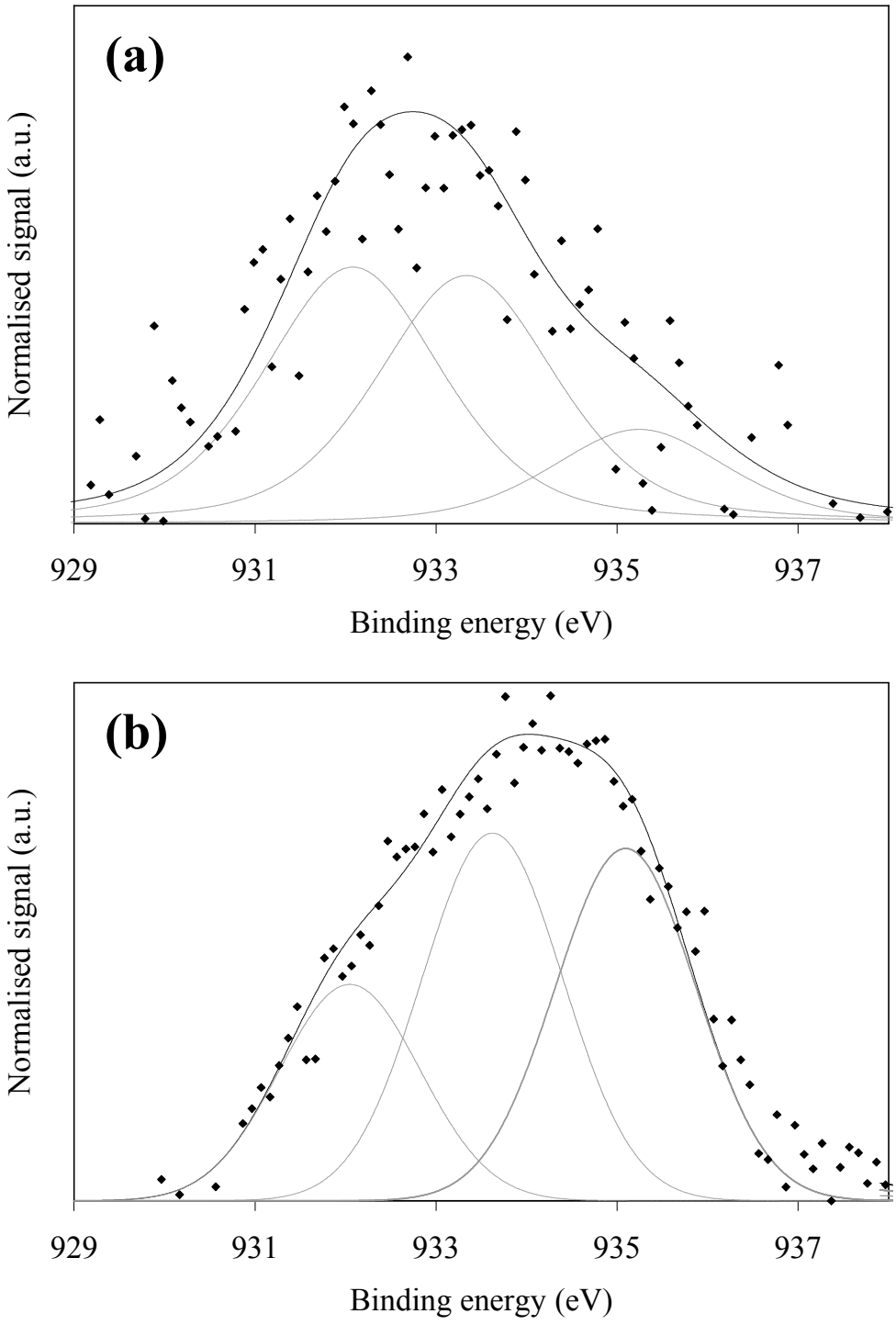
(a)
Normalised signal (a.u.)
929
931
933
935
937
Binding energy (eV)
(b)
Normalised signal (a.u.)
929
931
933
935
937
Binding energy (eV)

Figure 9.

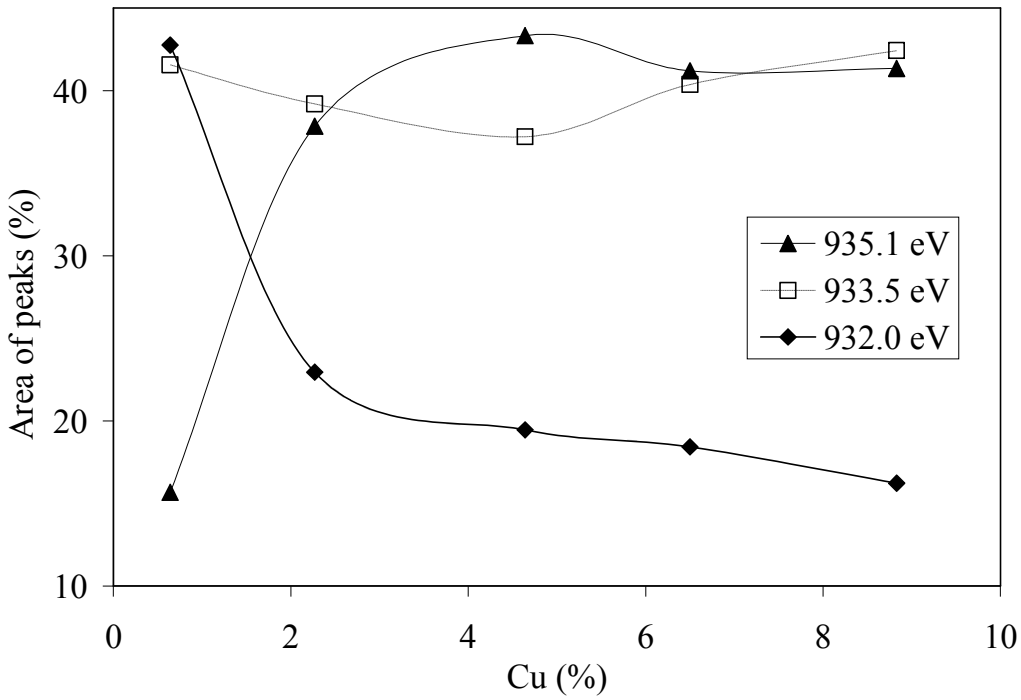

Figure 10.